

Equivalent Circuits for Nonuniform Transmission Line Simulation

Jacek Izydorczyk

Institute of Electronics
Silesian University of Technology, Akademicka 16, 44-100 Gliwice, Poland
jacek.izydorczyk@ieee.org

Abstract—The hereby article is devoted to elaboration of the analysis method of nonuniform transmission line (NUTL) with utilization of typical circuit simulator like SPICE. It is assumed that quasi-TEM modes are propagated in the NUTL. Solution of the problem is divided into three parts. 1) The analysis of nonuniform transmission line is reduced to the analysis of cascaded sections of linear varied nonuniform transmission line (LNLT). Proper algorithm originates from literature. 2) Computational model of linear varied nonuniform transmission line is elaborated following the asymptotic waveform evaluation methodology. The q -pole model is matched to imitate position of zeros and poles of admittance matrix of the NUTL. 3) Synthesis of passive circuit which implements the model for broad range values of LNLT slope constant. Consequently parameters of the circuit can be evaluated precisely as polynomial function of slope constant. Resultant model can be easily written in SPICE simulation language.

Index Terms—Asymptotic waveform evaluation, nonuniform transmission line, PR function, SPICE.

I. INTRODUCTION

Rapid development of VLSI technology yields large chips powered by a faster and faster external clock. Electrical length of interconnections becomes a significant fraction of a wavelength. Consequently conventional lumped-impedance models lead to a great computing complexity. There were many calculation models and techniques for real transmission lines that soften this problem. Most of them are focused on VLSI metal interconnections and connections between integrated circuits [1]. Unfortunately none of them can be easily implemented in a circuit simulator.

Strongly nonuniform transmission lines are used in microwave filters and impedance match circuits [6], to form impulse and to process quick-change signals [7]. Therefore, much attention has been paid to them [8], in recent times.

In this article, a new method of nonuniform transmission line (NUTL) simulation is proposed. The NUTL is divided into chunks approximated by lossless linear varied nonuniform transmission line (LNLT). For each approximating chunk an analytical solution of equations, which describes approximating LNLT is known. The solution is converted into SPICE acceptable macro-model [13] by methodology patterned on asymptotic waveform evaluation (AWE). In the original AWE method, initial conditions and a few first moments of the transient are matched with q -pole model. Herein a q -pole model is matched to imitate position and residues of poles and zeros of the admittance matrix of the LNLT. Proposed approximation methodology leads to the simulation model which is equivalent to a simple reciprocal circuit. Consequently, chunks of considerable length LNLT can be modeled with a low order ladder circuit. The model can be easily written in SPICE simulation language.

II. ANALYSIS OF NUTL

Text of this paragraph is quoted from [24] for completeness and smoothness of considerations. Consider ideal linear varied nonuniform transmission line (LNLT). Its wave impedance and propagation constant are:

$$Z(\xi) = Z_0(1 + k\xi), \quad \beta = \omega / c, \quad (1)$$

where Z_0 is a wave impedance in the beginning of the line, $k = (dZ(\xi)/d\xi)/Z_0$ is the slope constant, ξ is the position along the line, c is the phase speed of electromagnetic waves in the line, ω is the angular frequency of the waves. Solution of the telegraph equation for LNLT can be easily found in the

literature. For example in [26], the solution was found and elements of ABCD matrix have been given explicitly. Here the admittance matrix of LNTL line is used:

$$y_{11} = \frac{j}{Z_0} \cdot \frac{-J_0(x)Y_1(x(1+k\ell)) + J_1(x(1+k\ell))Y_0(x)}{J_1(x(1+k\ell))Y_1(x) - J_1(x)Y_1(x(1+k\ell))}, \quad (2)$$

$$y_{12} = y_{21} = \frac{-2 \cdot j/x(1+k\ell) / Z_0\pi}{\left[J_1(x(1+k\ell))Y_1(x) - J_1(x)Y_1(x(1+k\ell)) \right]}, \quad (3)$$

$$y_{22} = \frac{j/(1+k\ell)}{Z_0} \cdot \frac{-J_0(x(1+k\ell))Y_1(x) + J_1(x)Y_0(x(1+k\ell))}{J_1(x(1+k\ell))Y_1(x) - J_1(x)Y_1(x(1+k\ell))}. \quad (4)$$

where $J_n(x)$, $Y_n(x)$, are the Bessel function of the first and second kind of order n respectively; ℓ is the length of the line; $x = \omega\tau / k\ell$ and τ is delay time of the line and $j = \sqrt{-1}$. Using the solution, the following algorithm of NUTL analysis was formulated by K. Lu [26]. The algorithm is quoted here *in extenso*.

Step 1) "Numerically evaluate $y = \int_0^\xi d\xi / c(\xi)$.

Step 2) Select a set of points $(\xi_0, \xi_1, \dots, \xi_i, \dots, \xi_n)$ (corresponding to a set of points in terms of $y(\xi)$ $(y_0, y_1, \dots, y_i, \dots, y_n)$ in the region $0 \leq \xi \leq \ell$) so the NUTL is broken to small n sections. The $Z_c(y)$ of the i -th small section can be approximated by an LNTL:

$$Z_c(y) \approx \hat{Z}_c(y) = Z_c(y_i) [1 + k_i(y - y_i)], \quad (5)$$

$$\text{where } k_i = \frac{Z_c(y_{i+1}) - Z_c(y_i)}{Z_c(y_i)(y_{i+1} - y_i)}, \quad (6)$$

and $i = 0, 1, 2, \dots, n$

Step 3) Evaluate the ABCD matrix $[A^{i-th}]$ of the i -th section by using $\ell_i = y_{i+1} - y_i$, k_i , $Z_c(y_i)$ in place of ℓ , k , and Z_0 in (2)-(4).

Step 4) Evaluate the ABCD matrix $[A^{Total}]$ by cascading the $[A^{i-th}]$ for all small sections.

$$[A^{Total}] = \prod_{i=0}^n [A^{i-th}] \quad (7)$$

Step 5) After $[A^{Total}]$ is obtained, the S , Z , or Y parameters can be calculated by using matrix conversion."

The algorithm is biased by three drawbacks:

- The solution of telegraph equations is given in terms of the Fourier transform. Time domain solution needs one more step i.e. inverted Fourier transform. Practically only numerical approximation can be obtained by the means of FFT algorithm.
- The algorithm cannot be used directly to simulate nonlinear networks – that fact depreciates the value of the algorithm when simulation of digital circuits is considered.
- It cannot be implemented directly in circuit simulator for example in SPICE.

To alleviate these problems AWE approximation of LNTL chunks is considered in the next section.

III. LNTL ADMITTANCE MATRIX APPROXIMATION

Each formula (2)-(4) is approximated by rational function:

$$y_{ij} \approx \hat{y}_{ij} = \frac{a_0^{(ij)}}{x} + \sum_{n=1}^N \left(\frac{a_n^{(ij)}}{x - p_n} + \frac{a_n^{(ij)}}{x + p_n} \right), \quad (8)$$

where p_n are poles of y_{ij} numbered in ascending absolute value order and $a_n^{(ij)}$ is residue of y_{ij} at the pole p_n . Poles of all four admittance parameters of LNTL are the same and can be computed numerically as the solution of the equation:

$$J_1(x(1+k\ell))Y_1(x) - J_1(x)Y_1(x(1+k\ell)) = 0. \quad (9)$$

It is worth searching for the solution of the equation from the approximated value of the pole, which can be derived using approximation of the Bessel functions by trigonometric ones [30]:

$$p_n \approx \frac{n \cdot \pi}{k\ell}, \quad \text{where } n = \pm 1, \pm 2, \pm 3, \dots \quad (10)$$

The exact solution is obtained by the Newton-Raphson method. Residue $a_n^{(ij)}$ of y_{12} and y_{21} at poles p_n can be determined quite easily using the following formulae [33]:

$$a_n^{(12)} = a_n^{(21)} = \frac{-2j}{Z_0 \cdot \pi \cdot p_n (1+k\ell) M'(p_n, k\ell)}, \quad (11)$$

where $M'(x, k\ell)$ is derivative of left side of (9):

$$\begin{aligned}
M'(x, k\ell) &= J_2(x)Y_1(x(1+k\ell)) \\
&\quad - Y_2(x)J_1(x(1+k\ell)) \\
&\quad + (1+k\ell)J_1(x)Y_2(x(1+k\ell)) \\
&\quad - (1+k\ell)Y_1(x)J_2(x(1+k\ell)).
\end{aligned} \tag{12}$$

In case of parameters y_{12} and y_{21} , a simple cut of rational series expansion of (3) gives good results. A rational series expansion of (2) and (4) is also possible. Residue of y_{11} and y_{22} at poles p_n can be determined using the following equations:

$$a_n^{(11)} = \frac{[J_0(p_n)Y_1(p_n(1+k\ell)) - Y_0(p_n)J_1(p_n(1+k\ell))]}{j \cdot Z_0 \cdot M'(p_n, k\ell)}, \tag{13}$$

$$a_n^{(22)} = \frac{[Y_1(p_n)J_0(p_n(1+k\ell)) - J_1(p_n)Y_0(p_n(1+k\ell))]}{j \cdot Z_0 \cdot M'(p_n, k\ell)}. \tag{14}$$

Unfortunately, the rational approximation (8) obtained by the restriction of rational series expansion of (2) and (4) to first $N+1$ terms poorly approximate exact relations (2) and (4) in low frequency domain. A better idea is to find numerically, zeroes $x_n^{(11)}$ of y_{11} :

$$J_0(x)Y_1(x(1+k\ell)) - J_1(x(1+k\ell))Y_0(x) = 0 \tag{15}$$

and zeroes $x_n^{(22)}$ of y_{22} :

$$J_0(x(1+k\ell))Y_1(x) - J_1(x)Y_0(x(1+k\ell)) = 0. \tag{16}$$

In both cases, the approximate solution is:

$$x_n^{(11)} = x_n^{(22)} = \frac{n \cdot \pi + \pi / 2}{k\ell}, \tag{17}$$

where $n = 0, \pm 1, \pm 2, \pm 3, \dots$. The solution can be used to speed up the numerical search for an exact solution of (15) and (16). The goal is to obtain the approximation (8) by reproducing the exact location of first $2N+1$ poles and $2N$ zeroes of (2) and (4) respectively:

$$y_{ii} \approx \hat{y}_{ii} = Y_{ii} \frac{\prod_{n=1}^N (x - x_n^{(ii)}) (x + x_n^{(ii)})}{x \cdot \prod_{n=1}^N (x - p_n) (x + p_n)}. \tag{18}$$

Unknown parameter Y_{ii} should be chosen to reproduce the exact value of residuum $a_0^{(ii)}$ at pole $p_0=0$:

$$a_0^{(11)} = a_0^{(22)} = \frac{2j}{k\ell \cdot (2+k\ell)}. \tag{19}$$

This guarantees that the approximation (8) is accurate in the range of frequencies up to the last pole p_N . Formula for parameter Y_{ii} is as follows:

$$Y_{ii} = \frac{2j}{k\ell \cdot (2+k\ell)} \cdot \frac{\prod_{n=1}^N (p_n)^2}{\prod_{n=1}^N (x_n^{(ii)})^2}. \tag{20}$$

This way, we have an approximation of admittance parameters of linear varied nonuniform transmission line. The approximation consists of four formulas of the type (8). In case of parameters y_{12} and y_{21} residues are computed using (11). In case of y_{11} and y_{22} residues are computed as follows:

$$a_n^{(ii)} = \frac{j \cdot \prod_{m=1}^N |p_m|^2 \cdot \prod_{m=1}^N (p_m^2 + |x_m^{(ii)}|^2)}{p_n^2 (2+k\ell) k\ell \prod_{m=1}^N |x_m^{(ii)}|^2 \prod_{\substack{m=1 \\ m \neq n}}^N (p_m^2 - p_n^2)}. \tag{21}$$

The approximation circuit consists of four active circuits. Order of the whole circuit is four times higher than the order of the rational function used to approximate each individual parameter y_{ij} . Let us consider input admittance Y_{in} of the approximation circuit matched at the output:

$$Y_{in} = \frac{\hat{y}_{11} - Z_0(1+k\ell) \cdot (\hat{y}_{12}\hat{y}_{21} - \hat{y}_{11}\hat{y}_{22})}{1 + \hat{y}_{22}Z_0(1+k\ell)}. \tag{22}$$

The function is a rational function of frequency. Order of the function is $(2N+2)$ where N is the number of pole pairs taken into account in the formula (8). To obtain circuit of the order $2N+1$ determinant:

$$\Delta = \hat{y}_{12}\hat{y}_{21} - \hat{y}_{11}\hat{y}_{22} \tag{23}$$

could not possess poles of multiplicity two. Consequently, the relationship:

$$a_n^{(11)} a_n^{(22)} - (a_n^{(12)})^2 = 0 \text{ for } n=0, 1, \dots, N \tag{24}$$

must be fulfilled. Relationship (24) is true if we use (11), (13), and (14). But, when formulas (21), (11), and (22) are used to compute residues, then it is false.

IV. PASSIVE MODEL

Now the goal is to obtain an approximation circuit which is:

- as accurate as possible;
- order of the circuit should be $2N+1$ where N is the number of pole pairs taken into account in the formula (8);
- passive - to assure stability of every one model which contains the model of the nonuniform transmission line.

The conditions for a network with an admittance matrix $[y_{ij}(s)]$ to be passive are [14]:

1. $y_{ij}^*(s) = y_{ij}(s^*)$ for each pair ij (“*” is complex conjugate operator).
2. $[y_{ij}(s)]$ is a positive real (PR) matrix, i.e., the product $(\mathbf{z}^T)^* ([y_{ij}^*(s)]^T + [y_{ij}(s)]) \mathbf{z} \geq 0$ for all complex values of s with $\text{Re}(s) > 0$ and any arbitrary vector \mathbf{z} .

The first condition is satisfied whenever conjugate complex poles (zeros) are selected to create the model. The second condition is then equivalent to that all eigenvalues of $\text{Re}([y_{ij}(j\omega)])$ are greater than zero for $\omega \in \mathfrak{R} \cup \{\pm\infty\}$ [22]. Ensuring that condition is usually a challenging task because of all variations of Padé approximation are notoriously non-passive. Literature gives some ideas of how to reinforce passivity for models obtained by rational approximation of frequency domain responses and do not lose accuracy of approximation [14], and [16]. Nevertheless the model considered herein is free of such problems. Method of order reduction not only slightly enhances model accuracy but does not violate intrinsic model passivity. Therefore, it is sufficient to check passivity of the resulting model.

The idea of model order reduction is to slightly correct residuum $a_n^{(12)}$, computed by (11), and residues $a_n^{(11)}$ and $a_n^{(22)}$, computed by (21), to fulfill (24):

$$\hat{a}_n^{(11)} = a \cdot a_n^{(11)}, \hat{a}_n^{(22)} = b \cdot a_n^{(22)}, \hat{a}_n^{(12)} = c \cdot a_n^{(12)} \quad (25)$$

$$a \cdot b = \alpha^2 c^2 \quad \text{where} \quad \alpha^2 = \frac{(a_n^{(12)})^2}{a_n^{(11)} \cdot a_n^{(22)}}. \quad (26)$$

Correction coefficients a , b , and c should be as close to one as possible. For example, Euclidean distance should be as low as possible:

$$I(a, b, c) = (a - 1)^2 + (b - 1)^2 + (c - 1)^2. \quad (27)$$

Minimization of (27) with constraint (26) gives the solution:

$$a = \alpha \frac{1 + 2|\alpha|}{1 + 2\alpha^2} = b, \quad (28)$$

$$c = \frac{1 + 2|\alpha|}{1 + 2\alpha^2}. \quad (29)$$

After correction of residues, the input admittance Y_{in} of the approximation circuit is a rational function of order $2N+1$.

Passivity of the model can be assured by the checking of passivity criteria for the input impedance (22). A real rational function is the driving-point immittance of a linear, passive, lumped, reciprocal, and time one-port network if, and only if, it is a positive real. This condition can be formulated as the following theorem, cited from [23]:

Theorem 1. A rational function represented in the form

$$F(s) = \frac{P(s)}{Q(s)} = \frac{m_1(s) + n_1(s)}{m_2(s) + n_2(s)}, \quad (30)$$

where $m_1(s)$, $m_2(s)$ and $n_1(s)$, $n_2(s)$ are even and odd parts of the polynomials $P(s)$ and $Q(s)$, respectively, is positive real if, and only if, the following conditions are satisfied:

1. $F(s)$ is real when s is real;
2. $P(s) + Q(s)$ is strictly Hurwitz (zeroes lie on open left-hand plane);
- 3.

$$M(s^2) \Big|_{s=j\omega} = m_1(j\omega)m_2(j\omega) - n_1(j\omega)n_2(j\omega) \geq 0 \text{ for all } \omega.$$

The first condition is enforced by choosing of conjugate complex poles (zeros) of the model. The second condition can be checked by factorization of $P(s) + Q(s)$. The third condition can be reformulated in a much convenient form following [23]:

Theorem 2. If $M(s^2)$ is an even polynomial of a complex variable s with real coefficients and $M(0) > 0$ and $M(s)$ does not possess real negative roots then $M(s^2) \Big|_{s=j\omega} > 0$ for all ω .

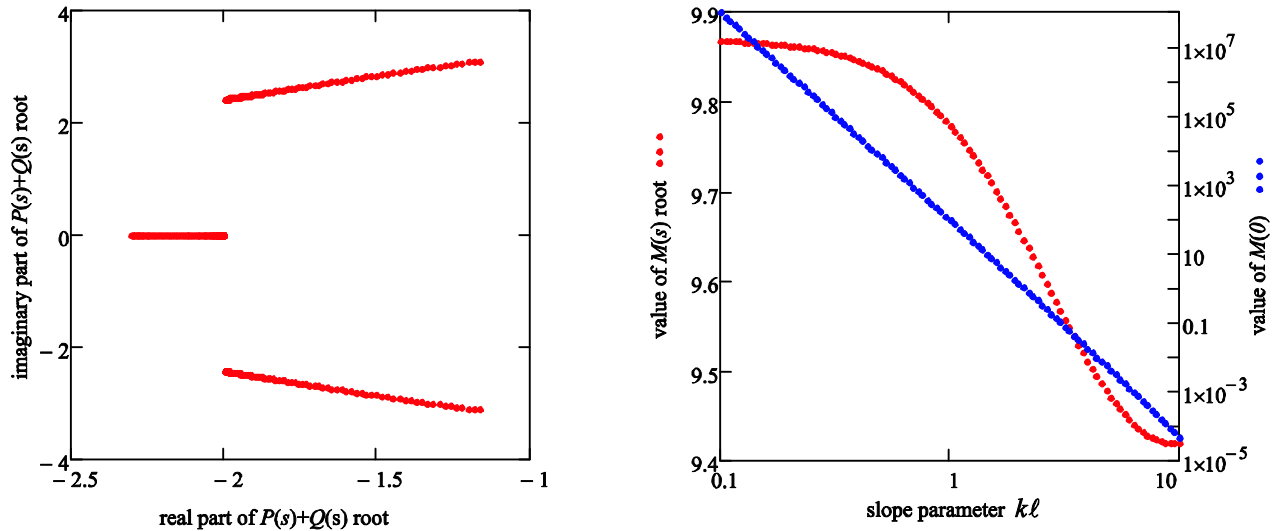


Fig. 1. Passivity check for third order model of LNTL: a) real vs. imaginary part of $P(s)+Q(s)$ roots; b) root of $M(s)$ (multiplicity two) and value $M(0)$.

Results of factoring polynomials $P(s)+Q(s)$ $M(s)$ and values $M(0)$ for the model of LNTL with parameter $N=1$ (third order) are shown in Fig.1. Factorization was performed for the value of the slope parameter kl lying in the range of 0.1 to 10. Polynomial $M(s)$ is a second order polynomial with only one root of multiplicity two. Each time the model passivity conditions are met.

Therefore, the admittance Y_{in} can be synthesized using Darlington methodology [34]. The synthesis algorithm is summarized in Appendix I. The algorithm is based on $Z=1/Y_{in}$ – input impedance of matched reciprocal circuit. For $N=1$, the result of the synthesis is particularly simple. The circuit approximating LNTL consists of inductance connected in series with Darlington C-type section – see Fig. 2. The synthesis has been conducted for normalized linear varied nonuniform transmission line described by parameter kl varied in relatively wide range from 0.1 to 10. The number of synthesized circuits was 100. For each of the inductance L_n , $n=1,3,4$; and for capacity C_2 , a discrete set of values was obtained depending on slope parameter kl . These values are arranged along the regression curves. Each inductance of the model depends on slope parameter kl almost linearly whereas variation of capacity C_2 can be estimated by rational function of second order. Consequently, a simple passive

approximation circuit can be formed. Inductances and capacitance of the subcircuit can be computed using the following equations:

$$L_1 = Z_0 \tau (6259 + (1152 - 6.943 \cdot kl) \cdot kl) \cdot 10^{-5}, \quad (31)$$

$$C_2 = \frac{\tau}{Z_0} \cdot \frac{(-0.4735 \cdot kl - 22.34) \cdot kl + 51.23}{(-11.13 \cdot kl + 1) \cdot kl + 51.27}, \quad (32)$$

$$L_3 = Z_0 \tau (3494 + (3188 + 8.580 \cdot kl) \cdot kl) \cdot 10^{-4}, \quad (33)$$

$$L_4 = Z_0 \tau (28796 + (3361 - 3.24 \cdot kl) \cdot kl) \cdot 10^{-5}. \quad (34)$$

Other configurations of the third order ($N=1$) lumped circuit, which models a section of the linear varied transmission line are discussed in [24].

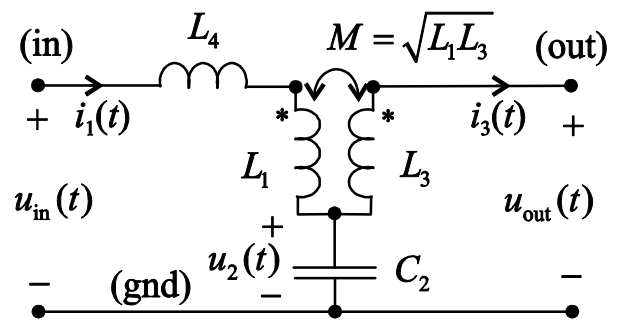


Fig. 2. Passive circuit, which models a segment of the linear varied nonuniform transmission line.

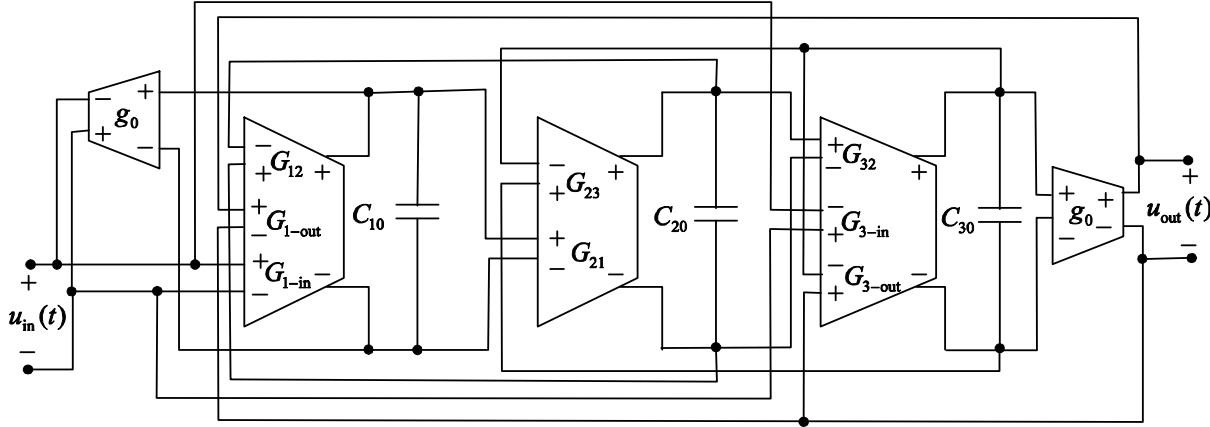


Fig. 3. Active circuit, which models a segment of the linear varied nonuniform transmission line.

Table 1: Transconductances of the active circuit modeling LNTL

Parameter	Expression
G_{12}	$\frac{(L_3 + \sqrt{L_1 \cdot L_3}) \cdot C_1}{L_3 \cdot L_4 \cdot g_0}$
G_{1-in}	$\frac{C_1}{L_4 \cdot g_0}$
G_{1-out}	$\frac{C_1 \cdot \sqrt{L_1 \cdot L_3}}{L_3 \cdot L_4 \cdot g_0}$
$G_{21} = G_{23}$	$\frac{C_2' \cdot g_0}{C_2}$
G_{32}	$\frac{(\sqrt{L_1 \cdot L_3} + L_1 + L_4) \cdot C_3}{L_3 \cdot L_4 \cdot g_0}$
G_{3-in}	$\frac{(\sqrt{L_1 \cdot L_3}) \cdot C_3}{L_3 \cdot L_4 \cdot g_0}$
G_{3-out}	$\frac{(L_1 + L_4) \cdot C_3}{L_3 \cdot L_4 \cdot g_0}$
g_0	an arbitrary value

V. SPICE MODEL

The passive circuit shown in Fig. 2 can be easily described in the SPICE simulation language. A convenient form of the description is a subcircuit. Values of inductance and capacitance, which compose the network, should be determined by the parameters passed to the subcircuit. If the used simulator has a preprocessor, that allows calculating the value of the subcircuit parameters

before analysis, then this task is relatively easy. Example of the model implementation in the form of subcircuit attributed by parameters, in the SPICE simulator environment, was presented in [24].

This article presents a concept of the model implementation, which does not require the involvement of the preprocessor. Many versions of SPICE, including many of those that come from the Berkeley version Spice3f, e.g. Ngspice program, does not have a preprocessor and does not allow user to define parameters. In this situation, parameters can be passed to subcircuit only in the form of voltages (currents) defined outside of the subcircuit. Voltages can easily modify the value of current sources – voltage controlled current sources. Much more difficult is to achieve the effect of modification of the capacity or inductance. As shown in the article [27], it is not impossible, but quite inconvenient. The technique proposed here is based on simulation of an analog computer, which is modeling a passive circuit from Fig. 2. Differential equations in normal form describing the circuit have the form:

$$\begin{bmatrix} \dot{u}_1(t) \\ \dot{u}_2(t) \\ \dot{u}_3(t) \end{bmatrix} = \begin{bmatrix} 0 & -\frac{T_3 + \sqrt{T_1 \cdot T_3}}{T_3 \cdot T_4} & 0 \\ \frac{1}{T_2} & 0 & -\frac{1}{T_2} \\ 0 & \frac{\sqrt{T_1 \cdot T_3} + T_1 + T_4}{T_3 \cdot T_4} & 0 \end{bmatrix} \begin{bmatrix} u_1(t) \\ u_2(t) \\ u_3(t) \end{bmatrix} +$$

Table 2: SPICE description of the active circuit modeling LNTL

```

.subckt xmachine.00 in gnd out gnd tau inz0 kL
*interface for parameters passing
Rtau tau tau2 10
vtau tau2 0 dc 0
rz0 inz0 0 1meg
rkL kL 0 1meg
*circuit reactances computing
VL1 100 0 dc 0
BL1 0 100 i=0.062591+(0.011523-6.942533e-5*v(kL,0))*v(kL,0)
VL3 200 0 dc 0
BL3 0 200 i=0.34938+(0.318778+8.58005e-4*v(kL,0))*v(kL,0)
VL4 300 0 dc 0
BL4 0 300 i=0.287957+(0.033614-3.240502e-5*v(kL,0))*v(kL,0)
VC2 400 0 dc 0
BC2 0 400 i=((-0.47351*v(kL,0)-22.34105)*v(kL,0)+51.22673)/((-
11.12705*v(kL,0)+1)*v(kL,0)+51.27397)
*analog computer
c10 1 gnd 20pF
c20 2 gnd 20pF
c30 3 gnd 20pF
b10 gnd 1 i=(1/i(VL4)*V(in,gnd)-
(i(VL3)+sqrt(i(VL1)*i(VL3)))/i(VL3)/i(VL4)*V(2,gnd)+sqrt(i(VL1)*i(VL3))/i(VL3)/i(VL4)*
b20 gnd 2 i=(1/i(VC2)*V(1,gnd)-1/i(VC2)*V(3,gnd))/i(vtau)*v(inz0)/250e
b30 gnd 3 i=(-sqrt(i(VL1)*i(VL3))/i(VL3)/i(VL4)*V(in,gnd)+
(sqrt(i(VL1)*i(VL3))+i(VL1)+i(VL4))/i(VL3)/i(VL4)*V(2,gnd)-
(i(VL1)+i(VL4))/i(VL3)/i(VL4)*V(out,gnd))/i(vtau)/v(inz0)
g1in in gnd 1 gnd 0.02
g2out gnd out 3 gnd 0.02
.ends

```

$$+ \begin{bmatrix} \frac{1}{T_4} & \frac{\sqrt{T_1 \cdot T_3}}{T_3 \cdot T_4} \\ 0 & 0 \\ -\frac{\sqrt{T_1 \cdot T_3}}{T_3 \cdot T_4} & -\frac{T_1 + T_4}{T_3 \cdot T_4} \end{bmatrix} \begin{bmatrix} u_{in}(t) \\ u_{out}(t) \end{bmatrix}, \quad (35)$$

where $\dot{u}_n(t)$ is time derivative of voltage $u_n(t)$ for $n=1,2,3$, $T_n = g_0 L_n$ for $n=1,3,4$, and $T_2 = C_2/g_0$. g_0 is an arbitrarily assumed value of trans-

conductance, while $u_1(t) = i_1(t)/g_0$ and $u_2(t) = i_2(t)/g_0$ are voltages derived from loop currents $i_1(t)$ and $i_2(t)$ marked in Fig. 2.

System of equations (35) can be realized in the form of the active circuit shown in Fig. 3. The circuit follows a typical active OTA filter based on “leapfrog” structure, though is not identical with the filter [28]. State variables are voltages on capacitors C_1 - C_3 . Relations between state variables, resulting from equations (35), are implemented by transconductances which value depends on three additional input voltages. The

Table 3: SPICE description of LNTL two segment model

```

.subckt xmachine.01 in gnd out gnd intau inz ink1x1.02 in
  gnd 2 gnd intau inz ink11 xmachine.00x2.02 2 gnd
  out gnd intau inz2 ink12 xmachine.00rk1 ink1 0
  1kbz2 inz2 0 v=v(inz,0)*(1+v(ink1,0)/2)bk11 ink11 0
    v=v(ink1,0)/2bk12 ink12 0
    v=v(ink1,0)/(2+v(ink1,0)).ends

```

parameters given in this way, modify the properties of the model by specifying a delay τ , wave impedance Z_0 , and slope parameter $k\ell$ of the line. The equations describing the individual transconductances are summarized in Table 1. In a case of typical OTA-based structure of “leapfrog” filter is enough to simulate an LC ladder biased by resistances [29]. Network from Fig. 3 can interact with any biasing system. State variables corresponding to the currents are transformed by the voltage-controlled current sources into corresponding currents actually observed at the ports of the network. As a result, such networks can be connected in a series to form the model of linearly varied transmission line of arbitrarily large order.

SPICE description of the circuit implementing the model in Fig. 3 is shown in Table 2. Input port of subcircuit named **xmachine.00** is between nodes **in** and **gnd**. Output port is between nodes **out** and **gnd**. Wave impedance of the line near the input port is equal Z_0 . Wave impedance of the line near the output port is equal $Z_0(1+k\ell)$. To obtain the appropriate circuit delay the current source should be inserted between the node **tau** and the ground (node number 0). Value of the source expressed in amperes should be equal to the line delay, expressed in nanoseconds. For example, if the line delay is intended to be 1ps, the current value generated by the source should be 1mA. Potential of **inz0** node (expressed in volts) defines the line impedance. Potential of **kl** node (expressed in volts) determines the slope parameter $k\ell$ of the transmission line. Only positive values of the slope parameter are valid.

VI. SIMULATIONS

Using third order circuit in Fig. 3, one could build LNTL model of arbitrarily high order. The idea is to use algorithm invented by K. Lu [26] and presented in section II. The LNTL is divided into small sections; each modeled using the circuit of Fig. 3. Admittance parameters of each section are reproduced by the model in wide range of frequencies. In particular, the mutual interaction of neighboring line segments is reproduced closely. The structure of the circuit causes, that mutually-far segments interact with each other poorly. As a result, it is expected that combining cascade circuits allows effective enhancement of model’s accuracy.

Table 3 shows how to declare a model of LNTL consisting of two segments of equal delay using SPICE simulation language. The first segment of the transmission line has a slope parameter equal to $k\ell/2$, where $k\ell$ is a slope parameter of entire LNTL. Input wave impedance of the first segment is Z_0 . The delay of this and the next segment is equal to $\tau/2$, where τ is a total delay of the LNTL. The appropriate value for this parameter is obtained by combining the **tau** nodes of both circuits and supplying an external source of current which defines total delay τ . The second segment is replaced by the circuit attributed by slope parameter $k\ell/(2+k\ell)$. Input impedance of the segment is equal $Z_0/(1+k\ell/2)$. By means of only ten subcircuits, similar to those in Table 3, one comes to the model of LNTL which consists of 1024 segments.

In order to examine the accuracy of the LNTL multi-segment model, the simulation experiment was conducted. The simulated circuit is

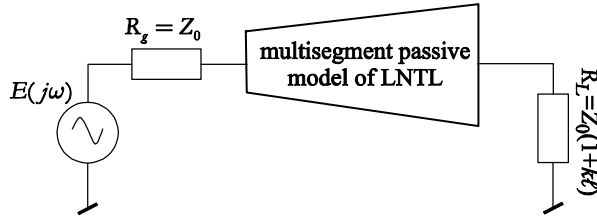


Fig. 4. Circuit used in simulation experiment for examination of LNTL model accuracy.

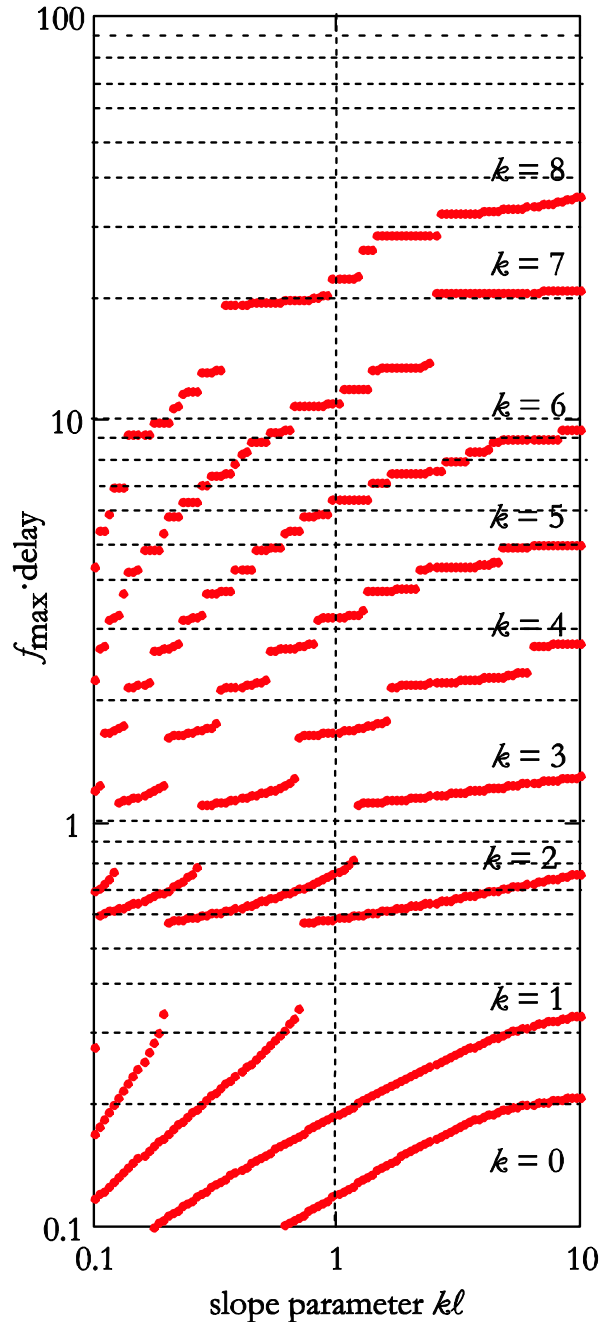


Fig. 5. Maximal frequency of the multi-segment LNTL model.

presented in Fig. 4. The input source (loading resistance) was matched to input (output) wave impedance of LNTL. The number of third order sections, LNTL model consists of, varied from 1 to 256. In each step of the experiment, the number of sections was doubled. In the experiment, the reflection coefficient of the input port $S_{11}(\omega)$ and the reflection coefficient of the output port $S_{22}(\omega)$ were studied. It was assumed, that input impedance of modeled transmission line is 50Ω , whereas delay of the line equal to 1 ns. The line slope parameter $k\ell$ has changed in the range of 0.1 to 10. The frequency response of the simulation model $S'_m(\omega)$, where $n=1, 2$, was compared with the response $S_m(\omega)$ obtained on the basis of analytical equations (2)-(4). This allowed to determine limit frequency f_{\max} , for each of the tested models, above which the relative deviation of the model reflection coefficient differs greater than 5% from the reflection coefficient determined analytically:

$$\max_{0 \leq \omega \leq 2\pi f_{\max}} \left| \frac{S_m(\omega) - S'_m(\omega)}{S_m(0)} \right| \leq 0.05. \quad (36)$$

We examined models consisting of sections, whose number K amounted to:

$$K = 2^k \quad \text{where } k=0,1,\dots,8. \quad (37)$$

Data for the SPICE program was prepared automatically, using an application written in LabVIEW[®] graphical language, due to the large number of test simulations. The results of the frequency domain analysis are shown in Fig. 5. The horizontal axis bears slope parameter $k\ell$ of the LNTL. The vertical axis bears the product of the maximal frequency f_{\max} and line delay. The set of curves is parameterized by variable k determining number of sections, which the model comprises. Figure 5 shows that the frequency range in which the model truly reflects the properties of the reflection coefficient is proportional to the number of sections used. The model is better when the transmission line is more nonuniform. This is successful information. The proposed model is useful wherever there is a line that shows high non-uniformity at a short distance compared to the line delay.

A circuit similar to the circuit presented in Fig. 4 was used to determine time complexity of

computations with model of the LNTL line. In this case, the linear varied transmission line described

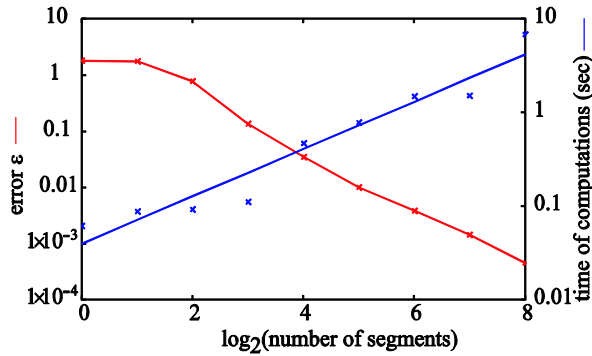


Fig. 6. Time domain error and time of computations versus number of third order segments the LNTL model consists of.

by the slope parameter $k\ell=10$ was used. The input port was excited by the time domain impulse rather than AC source. The impulse has shape of “raised cosine”:

$$e(t) = \frac{A}{2} \begin{cases} 1 - \cos(4\pi t / \tau) & \text{for } 0 \leq t \leq \tau/2 \\ 0 & \text{otherwise} \end{cases}, \quad (38)$$

where amplitude of the impulse was $A=1\text{V}$ and $\tau=1\text{ns}$ was the line delay. Duration of the impulse was equal to half of the line delay. The simulation objective was to obtain reflected wave from the input port in time range 0 to 2τ . Accuracy of the time domain simulation was determined by comparison of reflected wave $u'(t)$ computed by

SPICE, with the reflected wave $u(t)$ computed using analytical formulas (2)-(4). Error of the computations:

$$\varepsilon = \frac{\max_{0 \leq t \leq 2\tau} |u'(t) - u(t)|}{\max_{0 \leq t \leq 2\tau} |u(t)|}, \quad (39)$$

as a function of the LNTL model sections number is presented in Fig. 6. The latter figure, also, shows time of computations on a 2.5 GHz PC computer. The model, which consists of 16 segments gives error less than 4% , whereas computation time is no longer than 500ms.

VII. MEASUREMENTS

In order to verify the algorithm by experiment, the reflection coefficient of the input port $S_{11}(\omega)$ of nonuniform, asymmetric PCB stripline was measured. The transmission line under investigation was implemented on a conventional two-side epoxy-glass laminate. Thickness of the laminate dielectric layer is $h=1.5\text{mm}$. Copper foil thickness amount to $t=35\mu\text{m}$. Relative permittivity of the laminate dielectric layer is equal to $\varepsilon_p=4.2$. Line width varies continuously from 2.9 mm by 0.6 mm to 8.1 mm – see Fig. 7. The line is electrically matched on input and output port. Measurements were performed using the network analyzer HP4396A. Frequency range of the measurement spanned from 1.0 MHz to 1.8

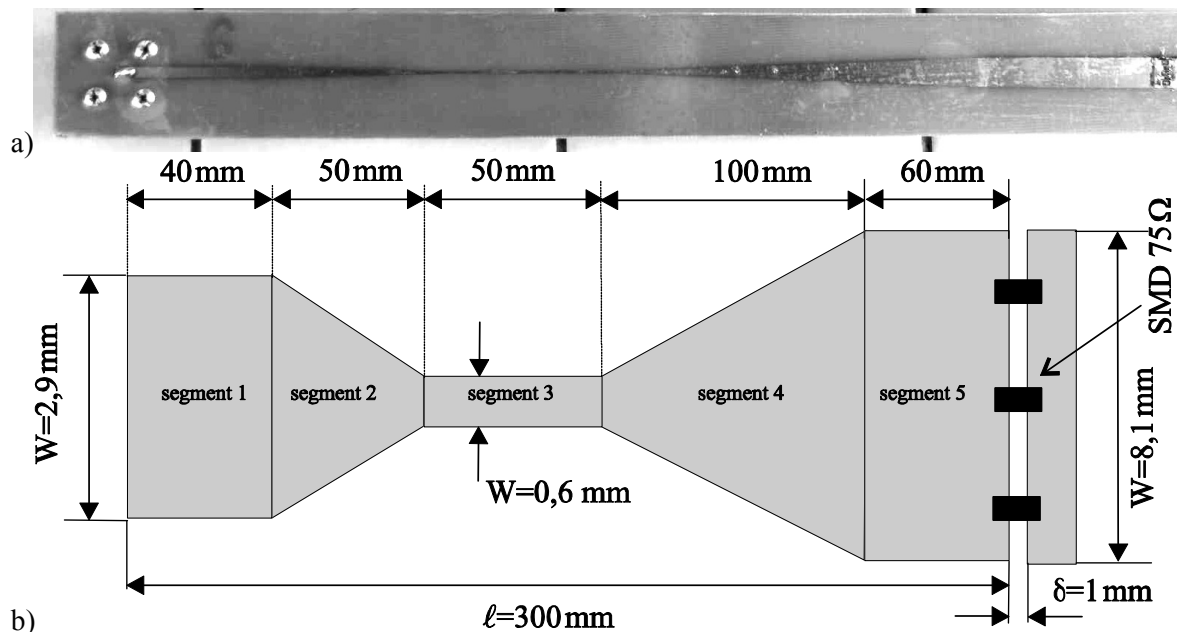


Fig. 7. Tapered lossless transmission lines investigated experimentally a) photograph b) drawing with dimensioning.

GHz. The amplitude and phase of the measured reflection coefficient of the input port is shown in Fig. 8.

The characteristic impedance of the line varies continuously from the value of about 50 ohms through 100 ohms to a value of approximately 25 ohms. However, there is not any generally accepted method of calculating the wave impedance stripline based on its geometry and electrical properties of materials. There are simplified equations, which do not take into account the thickness of the foil e.g. [31]. In literature one can find a more complex formula, which takes into account the thickness of the foil e.g. [32]. None of these equations are much better than the others. It was therefore decided that the characteristic impedance of the line calculated for the first time using the formula found in [31], and the second time using the model found in [32]. Then, the author made a model of nonuniform parts of the transmission line, as proposed in this article. Section 2 was modeled by four third-order segments. Section 4 was modeled by eight third-order segments. Uniform parts (segments 1, 3, and 5) were modeled by intristical SPICE model. The input port was excited by a triangular impulse. Basically, the shape of the impulse was the following:

$$e(t) = A \cdot \begin{cases} t/\tau_1 & \text{for } 0 \leq t \leq \tau_1 \\ (2\tau_1 - t)/\tau_1 & \text{for } \tau_1 \leq t \leq 2\tau_1, \\ 0 & \text{otherwise} \end{cases} \quad (40)$$

where $\tau_1 = 2$ ns and $A=1$ V. Pulse is formed through the Chebyshev filter of 15-order with a

pass-band frequency 1.8GHz, so to limit its spectrum. The wave reflected from the input port, as calculated by the program SPICE, is presented in the Fig. 9. Actually, the figure shows two waveforms computed by SPICE – time calculations was 1.02 s, using the SPICE program on a 2.5 GHz PC. First of them (solid line) concerns the profile of the transmission line impedance calculated by formulas from [32]. The second waveform (dotted line) concerns the impedance profile of transmission line calculated by formulas from [31]. In addition, the figure shows a reflected wave, which was calculated from the measured reflection coefficient (points). For calculations, the standard algorithm for convolution of discrete signals using the FFT was used [35]. Comparing the calculated and measured results, we found that the result agrees well with the experiment.

VIII. CONCLUSIONS

In this article, a method of nonuniform transmission line analysis is proposed. The method reduces NUTL to cascaded linear varied transmission lines. LNTL segments are approximated by a passive circuit, which consists of inductance, cascaded with Darlington C section. The model is implemented in circuit simulator as active circuit similar to OTA-based leapfrog filter. Parameters of each section are computed using polynomial regression. Cascaded circuits are insensitive to parameters variation. Due to this fact, inevitable regression errors do not disturb the frequency response of the model significantly.

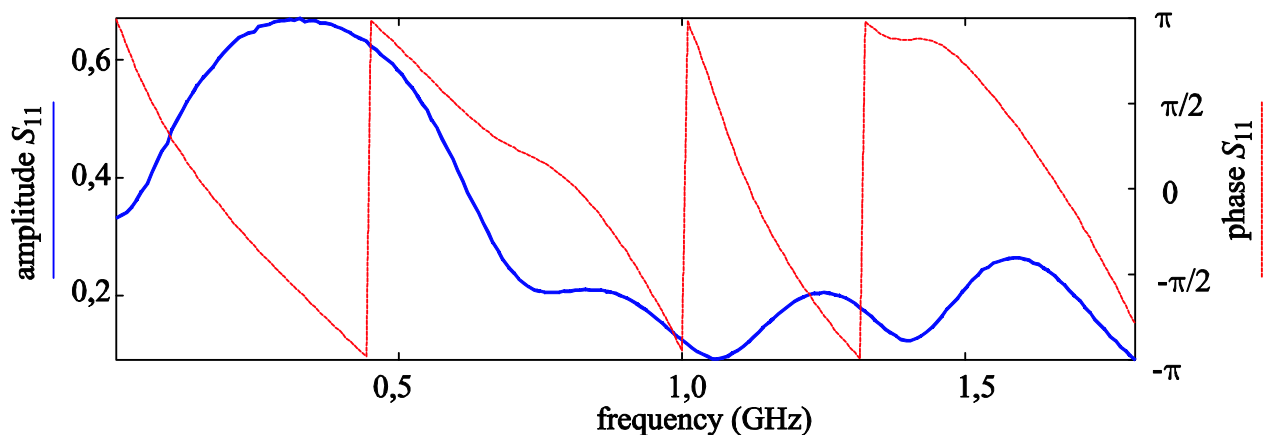


Fig. 8. Amplitude and phase of reflection coefficient $S_{11}(\omega)$ of stripline from Fig. 7. Measurement made with HP4396A.

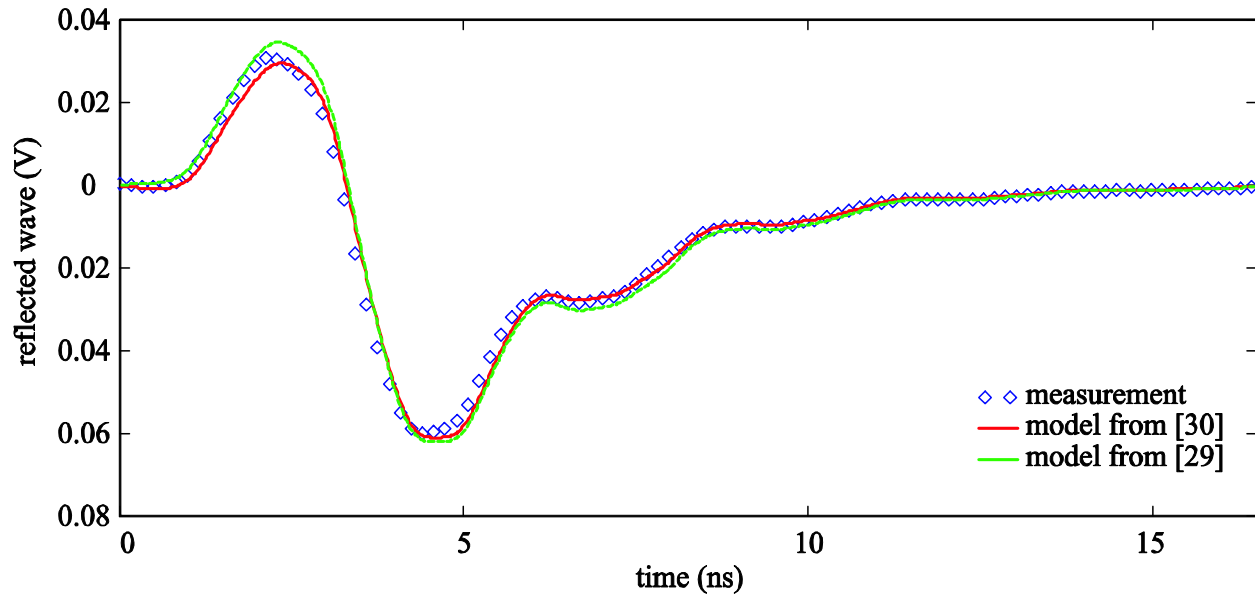


Fig. 9. Waveform, which was computed by SPICE, reflected from input port of the stripline (Fig. 7) vs. measured waveform.

Calculations performed using the proposed model agree well with laboratory measurements.

REFERENCES

- [1] J. Jeong and R. Nevels, "Time-Domain Analysis of a Lossy Nonuniform Transmission Line," *IEEE Transactions on Circuits and Systems II: Express Briefs*, vol. 56, no. 2, pp. 157–161, Feb. 2009.
- [2] L. Jia, W. Shi, and J. Guo, "Arbitrary-Difference Precise-Integration Method for the Computation of Electromagnetic Transients in Single-Phase Nonuniform Transmission Line," *IEEE Transactions on Power Delivery*, vol. 23, no. 3, pp. 1488–1494, July 2008.
- [3] M. Tang and J. Mao, "A Precise Time-Step Integration Method for Transient Analysis of Lossy Nonuniform Transmission Lines," *IEEE Transactions on Electromagnetic Compatibility*, vol. 50, no. 1, pp. 166–174, Feb. 2008.
- [4] E. Gad and M. Nakhla, "Simulation and sensitivity analysis of nonuniform transmission lines using integrated congruence transform," *IEEE Transactions on Advanced Packaging*, vol. 28, no. 1, pp. 32–44, Feb. 2005.
- [5] F. Kato, "A theory for deriving exactly solvable nonuniform transmission lines systematically," *IEEE Transactions on Circuits and Systems II: Express Briefs*, vol. 52, no. 12, pp. 836–840, Dec. 2005.
- [6] L. A. Hayden and V. K. Tripathi, "Nonuniformly coupled microstrip transversal filters for analog signal processing," *IEEE Trans. Microwave Theory Tech.*, vol. 39, pp. 47–53, Jan. 1991.
- [7] S. C. Burkhart and R. B. Wilcox, "Arbitrary pulse shape synthesis via nonuniform transmission lines," *IEEE Trans. Microwave Theory Tech.*, vol. 38, pp. 1514–1518, Oct. 1990.
- [8] G. Antonini, L. De Camillis, and F. Ruscitti, "A Closed-Form Sensitivity Analysis of Transmission Lines," *ACES Journal*, vol. 24, no. 4, pp. 352–360, Aug. 2009.
- [9] B. Essakhi, J. Benel, M. Smail, G. Akoun, and L. Pichon, "Circuit Models for Interconnects Using 3D Computational Techniques," *ACES Journal*, vol. 23, no. 1, pp. 39–45, March 2008.
- [10] A. G. Chiariello, A. Maffucci, G. Miano, F. Villone, and W. Zamboni, "High-Frequency Full-Wave Analysis of Interconnects with Inhomogeneous Dielectrics through an Enhanced Transmission Line Model," *ACES Journal*, vol. 23, no. 1, pp. 31–38, March 2008.
- [11] S. Barmada and M. Raugi, "Transient numerical solutions of nonuniform MTL equations with nonlinear loads by wavelet expansion in time or space domain," *IEEE Transactions on Circuits and Systems I: Fundamental Theory and Applications*, vol. 47, no. 8, pp. 1178–1190, Aug. 2000.
- [12] S. Barmada, "Algebraic solution of time-domain nonuniform transmission-line equations by 2-D wavelet transform," *IEEE Transactions on Circuits and Systems I: Fundamental Theory and Applications*, vol. 49, no. 4, pp. 504–508, Apr. 2002.

- [13] G.W. Roberts and A.S. Sedra, *SPICE, Second edition*, Oxford University Press, New York, 1997.
- [14] D. Saraswat, R. Achar, and M. S. Nakhla, "Global Passivity Enforcement Algorithm for Macromodels of Interconnect Subnetworks Characterized by Tabulated Data," *IEEE Transactions on Very Large Scale Integration (VLSI) Systems*, vol. 13, no. 7, pp. 819–832, July 2005.
- [15] P. Triverio, S. Grivet-Talocia, M. S. Nakhla, F. G. Canavero, and R. Achar, "Stability, Causality, and Passivity in Electrical Interconnect Models," *IEEE Transactions on Advanced Packaging*, vol. 30, no. 4, Nov. 2007, pp. 795–808.
- [16] D. Saraswat, R. Achar, and M. S. Nakhla, "Fast Passivity Verification and Enforcement via Reciprocal Systems for Interconnects with Large Order Macromodels," *IEEE Transactions on Very Large Scale Integration (VLSI) Systems*, vol. 15, no. 1, pp. 48–59, Jan. 2007.
- [17] B. Gustavsen and A. Semlyen, "Enforcing passivity for admittance matrices approximated by rational functions," *IEEE Transactions on Power Systems*, vol. 16, no. 1, pp. 97–104, Feb. 2001.
- [18] B. Porkar, M. Vakilian, R. Iravani, and S. M. Shahrtash, "Passivity Enforcement Using an Infeasible-Interior-Point Primal-Dual Method," *IEEE Transactions on Power Systems*, vol. 23, no. 3, pp. 966–974, Aug. 2008.
- [19] B. Gustavsen, "Fast Passivity Enforcement for S-Parameter Models by Perturbation of Residue Matrix Eigenvalues," *IEEE Transactions on Advanced Packaging*, vol. 33, no. 1, pp. 257–265, Feb. 2010.
- [20] B. Anderson, J. E. Bracken, J. B. Manges, G. Peng, and Z. Cendes, "Full-wave analysis in SPICE via model-order reduction," *IEEE Transactions on Microwave Theory and Techniques*, vol. 52, no. 9, pp. 2314–2320, Sept. 2004.
- [21] A. Lamecki and M. Mrozowski, "Equivalent SPICE Circuits With Guaranteed Passivity from Nonpassive Models," *IEEE Transactions on Microwave Theory and Techniques*, vol. 55, no. 3, pp. 526–532, March 2007.
- [22] W. Cauer, *Synthesis of Linear Communications Network*, New York: McGraw-Hill, 1958.
- [23] W-K. Chen, "Passive Immittances and Positive-Real Functions," *The Circuits and Filters Handbook*, CRC Press Inc., Boca Raton, 2003.
- [24] J. Izydorczyk, "A simple SPICE model of a nonuniform transmission line," *33rd International Conference and Exhibition IMAPS – Poland 2009*, Gliwice-Pszczyna, pp. 163–166, 21-24 September 2009.
- [25] J. Izydorczyk, "Nonuniform transmission line simulation with circuit simulator," *Proceedings of IEEE MELECON 2010 Mediterranean Electrotechnical Conference*, Valetta (Malta), 25-28 April 2010.
- [26] K. Lu, "An Efficient Method for Analysis of Arbitrary Nonuniform Transmission Lines," *IEEE Trans. Microwave Theory Tech.*, vol. 45, no. 1, pp. 9–14, January 1997.
- [27] G. J. Fisher and J. A. Connelly, "Modeling Time-Dependent Elements for SPICE Transient Analyses," *IEEE Transactions on Computer-Aided Design of Integrated Circuits and Systems*, vol. 5, no. 3, pp. 429–432, July 1986.
- [28] E. Sanchez-Sinencio and J. Silva-Martinez, "CMOS transconductance amplifiers, architectures and active filters: a tutorial," *IEE Proceedings - Circuits, Devices and Systems*, vol. 147, no. 1, pp. 3–12, Feb 2000.
- [29] R. Schaumann, "Continuous-Time Integrated Filters," *The Circuits and Filters Handbook*. CRC Press, Boca-Raton, 2003.
- [30] N. W. McLachlan, *Bessel Functions for Engineers*, 2nd edition, Clarendon Press, Oxford, 1955.
- [31] S. Rosłonec, *Design methodology of some linear microwave circuits*, WKiŁ, Warszawa, pp. 125–128, 1987.
- [32] T. K. Ishii, "Transmission lines," *The Circuits and Filters Handbook*. CRC Press and IEEE Press, 2003, pp. 1165–1181.
- [33] T. Needham, *Complex Analysis*, Oxford University Press, Oxford, 2002.
- [34] H. J. Carlin, "Darlington synthesis revisited," *IEEE Trans. Circuits Syst. I*, vol. 46, no. 1, pp. 14–21, January 1999.
- [35] A.V. Oppenheim and R. W. Schaffer, *Digital Signal Processing*, Prentice-Hall. Inc., Englewood Cliffs, New Jersey, 1975.

Appendix I

Synthesis algorithm of Nth order model of LNTL

1. Let delay of the line τ be equal to 1s and let wave impedance at the input Z_0 of the line be equal to 1Ω .
2. Select a set of points $\{k\ell_1, k\ell_2, \dots, k\ell_K\}$ from the interval $0.1 \leq k\ell \leq 10$.
3. $n = 1$.
4. Let $k\ell = k\ell_n$.
5. Numerically evaluate $2N+1$ poles of the linear varied nonuniform transmission line. Pole is always at $\omega = 0$. The rest of $2N$ poles are solutions of the following nonlinear equation:

$$J_1\left(\frac{p(1+k\ell)}{k\ell}\right)Y_1\left(\frac{p}{k\ell}\right) - J_1\left(\frac{p}{k\ell}\right)Y_1\left(\frac{p(1+k\ell)}{k\ell}\right) = 0.$$

The solutions should have the smallest absolute value possible. Approximate values of the solutions are given by formula $p \approx n \cdot \pi$ where $n = \pm 1, \pm 2, \dots, \pm N$.

6. Evaluate residues of y_{21} parameter at poles found in Step 4) by using equation (11).

7. Numerically evaluate $2N$ zeroes of y_{11} parameter and $2N$ zeroes of y_{22} parameter of the linear varied nonuniform transmission line. Zeros of y_{11} parameters are solutions of nonlinear equation:

$$J_1\left(\frac{p(1+k\ell)}{k\ell}\right)Y_0\left(\frac{p}{k\ell}\right) - J_0\left(\frac{p}{k\ell}\right)Y_1\left(\frac{p(1+k\ell)}{k\ell}\right) = 0.$$

Zeros of y_{22} parameter are solutions of nonlinear equation:

$$J_1\left(\frac{p}{k\ell}\right)Y_0\left(\frac{p(1+k\ell)}{k\ell}\right) - J_0\left(\frac{p(1+k\ell)}{k\ell}\right)Y_1\left(\frac{p}{k\ell}\right) = 0$$

Approximate values of zeros are given by formula $p \approx n \cdot \pi + \pi/2$ where $n = -N, -N+1, \dots, N-1$.

8. Evaluate residues of y_{11} and y_{22} parameter at poles found in Step 4) by using equation (13) and (14) respectively.

9. Evaluate correction coefficients a, b and c for each residuum by using formulas (28) and (29).

10. Evaluate coefficients of rational function, which describes the input impedance $Z(s) = 1/Y_{in}(s)$ by using equation (22).

Determinant $\Delta = y_{12}^2 - y_{11}y_{22}$ possess only poles of multiplicity one. Residuum a_n of the determinant at pole p_n can be computed using formula:

$$a_n = \sum_{\substack{k=-N \\ k \neq n}}^N \frac{2a_{k,12}a_{n,12} - a_{k,22}a_{n,11} - a_{n,22}a_{k,11}}{(p_k - p_n)}.$$

where $a_{n,ij}$ is a corrected residuum of y_{ij} at pole p_n .

11. Separate inductance L_x using formula:

$$L_x = \lim_{s \rightarrow \infty} \frac{Li(s)}{s \cdot Mn(s)}, \quad (41)$$

where impedance function is a ratio of polynomials $Z(s) = Li(s)/Mn(s)$.

12. Let us $Z(s) \leftarrow Z(s) - sL_x$.

13. Numerically solve polynomial equation:

$$Ev(Z(s)) = 0. \quad (42)$$

14. Choose solution s_0 of (42) which has negative real part and minimal absolute value.

15. Evaluate index set $\{q_0, q_1, q_2, q_3\}$ assigned to s_0 by impedance function $Z(s)$. Elements of index set are given by formulas:

$$q_0 = \frac{R_0/\sigma_0 - X_0/\omega_0}{R_0/\sigma_0 + X_0/\omega_0}, \quad (43)$$

$$q_1 = \frac{2Z_0Z_0^*}{R_0/\sigma_0 + X_0/\omega_0}, \quad (44)$$

$$q_2 = \frac{2}{R_0/\sigma_0 - X_0/\omega_0}, \quad (45)$$

$$q_3 = \frac{R_0/\sigma_0 + X_0/\omega_0}{R_0/\sigma_0 - X_0/\omega_0} = \frac{1}{q_0}, \quad (46)$$

$$\text{where } Z(s_0) = Z_0 = R_0 + j \cdot X_0. \quad (47)$$

16. Compute coefficients of rational function:

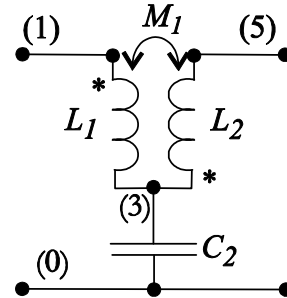


Fig. 10. The Darlington type-C section.

$$W_1(s) = \frac{D_1(s)Z(s) - B_1(s)}{-C_1(s)Z(s) + A_1(s)}, \quad (48)$$

$$\text{where } A_1(s) = q_3s^2 + s_0s_0^*, \quad (49)$$

$$B_1(s) = q_1s, \quad (50)$$

$$C_1(s) = q_2s, \quad (51)$$

$$D_1(s) = q_0s^2 + s_0s_0^*. \quad (52)$$

Detailed algorithm of computations is given in the Appendix II.

17. If s_0 is a real function, compute parameters of type-C section:

$$L_1 = \frac{1}{q_0q_2}, \quad L_2 = \frac{q_0}{q_2}, \quad (53)$$

$$C_2 = \frac{q_2}{\sigma_0^2}, \quad M_1 = \frac{-1}{q_2} < 0. \quad (54)$$

18. If order of $W_1(s)=0$ then go to 25.
19. Let $Z(s) \leftarrow W_1(s)$.

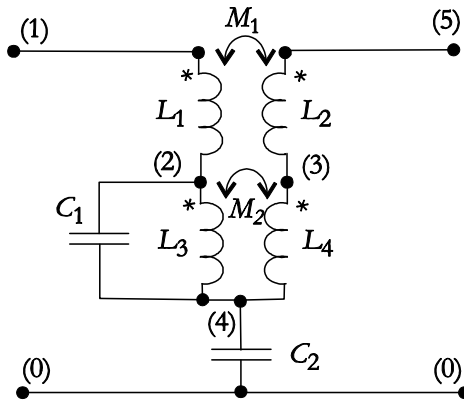


Fig. 11. The Darlington type-D section

20. Evaluate index set $\{p_0, p_1, p_2, p_3\}$ assigned to s_0 by modified impedance function $Z(s)$ by using equations (43)-(47).

21. Compute coefficients of rational function:

$$W_2(s) = \frac{D_2(s)Z(s) - B_2(s)}{-C_2(s)Z(s) + A_2(s)}, \quad (55)$$

$$\text{where } A_2(s) = p_3s^2 + s_0s_0^*, \quad (56)$$

$$B_2(s) = p_1s, \quad (57)$$

$$C_2(s) = p_2s, \quad (58)$$

$$D_2(s) = p_0s^2 + s_0s_0^*. \quad (59)$$

Detailed algorithm of computations is given in the Appendix II.

22. Compute parameters of type-D section:

$$L_1 = \frac{p_3q_3}{p_3q_2 + p_2q_0}, \quad L_2 = \frac{p_0q_0}{p_3q_2 + p_2q_0}, \quad (60)$$

$$M_1 = \sqrt{L_1L_2}, \quad C_2 = \frac{p_2 + q_2}{s_0s_0^*}, \quad (61)$$

$$M_2 = -\frac{\omega_{13}^4 - 2(\omega_0^2 - \sigma_0^2)\omega_{13}^2 + |s_0|^4}{\omega_{13}^4(p_3q_2 + p_2q_0)} \leq 0, \quad (62)$$

$$\text{where } \omega_{13}^2 = \frac{s_0s_0^*(p_2 + q_2)}{p_3q_2 + p_2q_0}, \quad (63)$$

$$L_4 = -\frac{q_2M_2}{p_2}, \quad L_3 = -\frac{p_2M_2}{q_2}, \quad C_1 = -\frac{q_2}{\omega_{13}^2p_2M_2}. \quad (64)$$

23. If order of $W_2(s)=0$ then go to 25.
24. Let $Z(s) \leftarrow W_2(s)$ and go to 13.

25. Let $n = n + 1$.
26. If $n \leq N$ go to 4.
27. For each element of the circuit, find parameters of regression curve describing variation of the element versus variations of kl parameter.

Appendix II

Algorithm of rational function separating

Consider rational PR function

$Z(s) = Li(s) / Mn(s)$, where

$$Li(s) = l_0 + l_1s + \dots + l_Ns^N,$$

$Mn(s) = m_0 + m_1s + \dots + m_Ns^N$ and four polynomials:

$$A(s) = a_0 + a_2s^2, \quad B(s) = b_1s, \quad (65)$$

$$C(s) = c_1s, \quad D(s) = d_0 + d_2s^2,$$

obtained according equations (49)-(52). Exists rational PR function $W(s)$ [34]:

$$Z(s) = \frac{A(s)W(s) + B(s)}{C(s)W(s) + D(s)} \quad (66)$$

$$\text{or } Z(s) = \frac{A(s)Li'(s) + B(s)Mn'(s)}{C(s)Li'(s) + D(s)Mn'(s)} = \frac{Li(s)}{Mn(s)}, \quad (67)$$

where $Li'(s) = l'_0 + l'_1s + \dots + l'_{N-1}s^{N-1}$, $Mn'(s) = m'_0 + m'_1s + \dots + m'_{N-1}s^{N-1}$. Order of $W(s)$ is equal to order of $Z(s)$ decremented by 2. Coefficients of the left side numerator should be equal the right side coefficients of numerator of (67). At the same time, coefficients of the left side denominator of should be equal coefficients of the right side denominator of (67). From equality of free coefficients we obtain:

$$l'_0 = \frac{l_0}{a_0}, \quad m'_0 = \frac{l'_0}{d_0}. \quad (68)$$

Equality of first order coefficients gives:

$$l'_1 = \frac{l_1 - m'_0b_1}{a_0}, \quad m'_1 = \frac{m_1 - l'_0c_1}{d_0}. \quad (69)$$

Equality of second order coefficients gives:

$$l'_2 = \frac{l_2 - m'_1b_1 - l'_0a_2}{a_0}, \quad m'_2 = \frac{m_2 - l'_1c_1 - m'_0d_2}{d_0}. \quad (70)$$

Equality of third order coefficients gives:

$$l'_3 = \frac{l_3 - m'_2b_1 - l'_1a_2}{a_0}, \quad m'_3 = \frac{l_3 - l'_2c_1 - m'_1d_2}{d_0}. \quad (71)$$

In general, following recursive formula can be written:

$$l_k = \frac{l_k - m'_{k-1}b_1 - l'_{k-2}a_2}{a_0},$$

$$m_k = \frac{m_k - l'_{k-1}c_1 - m'_{k-2}d_2}{d_0},$$
(72)

where $k = 0, 1, \dots, N-1$. Initial conditions for computations are:

$$l_{-1} = l_{-2} = m_{-1} = m_{-2} = 0. \quad (73)$$

Similarly, the reverse computing formula can be obtained.



Jacek Izydorczyk (M'95) was born in Bielszowice, Silesia, Poland in 1964 and became a Member (M) of IEEE in 1995 and senior member of IEEE in 2009.

He obtained his M.S. degree from Silesian University of Technology, Gliwice, Poland in 1988, Ph.D. degree from Silesian University of Technology, Gliwice, Poland in 1990. His dissertation research dealing with the construction of time domain invariants of sensitivities in the linear and non-linear circuits. He is involved in the researches dealing with network invariants, circuit simulations, magnetic media modeling, signal processing, speech synthesis, speech modeling, and analog filters.

Dr. Izydorczyk is author or co-author of three books published in Poland, i.e. *Pspice*, *Signal Theory*, and *Analog and Digital Filters*.